Direct measurement of the intermolecular forces between counterion-condensed DNA double helices

Evidence for long range attractive hydration forces

Donald C. Rau and V. Adrian Parsegian

Laboratory of Biochemistry and Metabolism, National Institute of Diabetes and Digestive and Kidney Diseases; and Physical Sciences Laboratory, Division of Computer Research and Technology, National Institutes of Health, Bethesda, Maryland 20892

ABSTRACT Rather than acting by modifying van der Waals or electrostatic double layer interactions or by directly bridging neighboring molecules, polyvalent ligands bound to DNA double helices appear to act by reconfiguring the water between macromolecular surfaces to create attractive long range hydration forces. We have reached this conclusion by directly measuring the repulsive forces between parallel B-form DNA double helices pushed together from the separations at which they have self organized into hexagonal arrays of parallel rods. For all of the wide variety of "condensing agents" from divalent Mn to polymeric protamines, the resulting intermolecular force varies exponentially with a decay rate of 1.4–1.5 Å, exactly one-half that seen previously for hydration repulsion. Such behavior qualitatively contradicts the predictions of all electrostatic double layer and van der Waals force potentials previously suggested. It fits remarkably well with the idea, developed and tested here, that multivalent counterion adsorption reorganizes the water at discrete sites complementary to unadsorbed sites on the apposing surface. The measured strength and range of these attractive forces together with their apparent specificity suggest the presence of a previously unexpected force in molecular organization.

INTRODUCTION

For their ability to create strong and specific associations under exquisite control, the forces between and within macromolecules have long been recognized as a key to the regulation of cellular activity. Yet, while the importance of intermolecular forces in macromolecular organization is well recognized, it is not generally apparent that traditional theories of such forces are inadequate. Direct measurement of interactions between membranes and between macromolecules has shown that, in the crucial last 10 Å of separation, forces of solvation are far more important than the electrostatic and van der Waals forces traditionally assumed to act between charged or polar surfaces. It is now beginning to emerge that these "hydration" forces can confer the strength, specificity, and control required for macromolecular assembly.

To our knowledge, there is still only one way to measure directly the forces between macromolecules in solution. That is to create ordered arrays of repelling molecules and to use x-ray diffraction to measure the change in intermolecular spacing with applied osmotic stress. Besides obtaining molecular force versus separation curves, one can sometimes also measure the change in molecular configurational entropy with separation (Podgornik et al., 1989). Through use of this Osmotic Stress Method (Parsegian et al., 1986), there are now data on forces between a large variety of phospholipid bilayers (e.g., Rand, 1981; Rand and Parsegian, 1989), between DNA double helices (Rau et al., 1984), between neutral and charged polysaccharides (Rau and Parsegian, 1990), and on inverted hexagonal phases of phospholipids (Rand et al., 1990). Osmotic stress has been used as well to create a phase diagram of an assembling protein (Prouty et al., 1985) and to measure the internal volume change in voltage-gated transmembrane ionic channels (Zimmerberg and Parsegian, 1986). To the extent that one can compare results with force balance measurements between macroscopic surfaces (e.g., Horn et al., 1988), there is excellent agreement between macroscopic and molecular methods of measurement. Few systems are as well suited to osmotic stress measurements as ordered assemblies of DNA (Rau et al., 1984).

Used as a model for cellular and viral packing of DNA (Wilson and Bloomfield, 1979; Widom and Baldwin, 1980; Chattoraj et al., 1978), poised with the order required for direct force measurement (Schellman and Parthasarathy, 1984), regulated by controlled exposure to different kinds of ion (Wilson and Bloomfield, 1979; Gosule and Schellman, 1978; Widom and Baldwin, 1983), and made from molecules of robust well defined structure, the spontaneously forming arrays of ligand-condensed DNA are ideal for examining the kinds of interactions that can occur between large molecules. X-ray diffraction by these compact structures reveals hexagonal arrays of parallel double helices with interaxial distances 6–12 Å greater than the 20-Å helical diameter (Schellman and Parthasarathy, 1984). Until now, studies have emphasized the requirements for condensation (ligand activity, temperature, solvent com-

position, activity of non-condensing salts) to gather information on mechanisms. Here, because parallel double helices are not condensed to contact, we have measured the repulsive forces between helices as they are brought together from their spontaneously-assumed spacings. These measured forces allow one to inquire systematically into the balance of attractive and repulsive forces that creates these minimum energy spacings.

We find that these forces are neither consistent with any model of direct ionic bridging nor with a balance of electrostatic/hydration repulsion against van der Waals attraction. Rather, the evidence is for an attractive form of the hydration force. Rearrangement or release of water about the adsorbing ionic ligand and the host double helix is driven in part by the entropy of solvent release (Rau and Parsegian, 1992), a kind of "hydrophobic interaction" between polar surfaces.

After collapse under these attractive forces, the ~3 Å decay length exponential repulsion seen between double helices in ordinary solutions is replaced by a ~1.5-Å decay force regardless of the kind of condensing ion even though the magnitudes of forces change dramatically with condensing ion species. The striking halving of the decay length can be rationalized by simple modification of the formalism developed for purely repulsive hydration forces. The mutual dependence of condensation on applied osmotic stress and ion activity allows one to measure the number of ions bound or rearranged upon condensation as well as to estimate the strength of attractive forces that drive assembly.

MATERIALS AND METHODS

Materials and chemicals

Spermidine trihydrochloride and salmon protamine were obtained from Sigma Chemical Co. (St. Louis, MO); cobaltic hexammine chloride ($Co(NH_3)_6Cl_3$) from Eastman-Kodak Co. (Rochester, NY); and manganese perchlorate ($Mn(ClO_4)_2$) from Aldrich Chemical Co. (Milwaukee, WI). All were used without further purification. Polyethylene glycols (PEG), average molecular weights 8,000 and 20,000, were purchased from Sigma Chemical Co. PEG was used without further purification for most experiments. Some control experiments were done, however, with PEG 20,000 average molecular weight that had been dissolved in water, dialyzed against distilled water, with several changes, for ~24 h (Spectra-Por dialysis membranes with a 6,000–8,000 molecular weight cutoff) to remove low molecular species and contaminants, and lyophilized to dryness. There was no observable difference between results obtained with untreated and dialyzed PEGs. High molecular weight DNA was prepared from adult chicken whole blood as described by (McGhee et al., 1981), and exhaustively dialyzed against 10 mM TrisCl (pH 7.5), 1 mM EDTA.

Osmotic stress

The osmotic stress technique applied to DNA has been described in detail elsewhere (Rau et al., 1984; Parsegian et al., 1986; Podgornik et al., 1989). The method is schematically illustrated in Fig. 1. Only briefly here, we take advantage of the ability of PEG in aqueous solutions to phase separate from DNA. Water and small ions are free to move between the PEG and DNA phases, establishing an equilibrium distribution, which we assume means the activity of water and small ions is the same in the PEG and DNA phases. The PEG is excluded from the DNA phase and exerts an osmotic pressure on it. At equilibrium, the distance between helices, measured by x-ray diffraction is determined by a balance of the expansive force due to interhelix repulsion and the compressive osmotic stress from the bathing PEG solution. In univalent salt solution, the phase separation of DNA and PEG simply means that DNA–DNA interactions are less repulsive than DNA–PEG interactions, not that helices are absolutely attractive. The separation can be artificially imposed by a dialysis membrane (1,000 molecular weight cutoff) between the PEG solution and the DNA pellet, with no direct contact between the two polymers, as shown in Fig. 1. Interhelical distances are unchanged with or without a membrane. PEG solution osmotic pressures, as a function of weight percent concentration, are given in Parsegian et al. (1986). The osmotic pressure of a 20% PEG (8,000 MW) solution in 0.25 M NaCl is within 10% of the osmotic pressure in water as measured by a membrane osmometer (with a 500 MW cutoff membrane). Salt does not seem to have a significant effect on PEG osmotic pressure. Additionally, the osmotic pressure of the 20% PEG solution in 0.25 M NaCl measured by a Wescor vapor pressure osmometer (model 5100C) is within 10% of the sum of the separately measured osmotic pressures of a 20% PEG solution in water and of a 0.25 M NaCl solution. PEG does not seem to have a significant effect on salt activity.

Precipitated DNA pellets (~300 μg of DNA) are prepared either by direct ethanol precipitation in 0.3 M NaCl, by precipitation with the polyvalent ion of interest, or by phase separation from 5% PEG solutions in 0.5 M NaCl. These pellets are then equilibrated against PEG solutions (~1 ml volume) of different weight concentrations prepared by dissolving PEG in aqueous salt solutions of fixed ionic (NaCl and polyvalent ion) composition. Solutions are buffered at ~pH 7.5 with either 10 mM Tris-Cl or 10 mM Hepes. The bathing PEG-salt medium over the pellet is changed several times over the course of ~2 wk to ensure equilibration. The protocol for preparation of protamine-assembled samples was somewhat different because protamine is not soluble at high PEG concentrations. DNA was slowly titrated with a 1 mg/ml protamine solution in 0.2 M NaCl, 10 mM TrisCl, until complete precipitation. The DNA is pelleted by centrifugation, washed once with cold 10 mM TrisCl, then equilibrated against PEG solutions containing 10 mM TrisCl, with no added protamine.

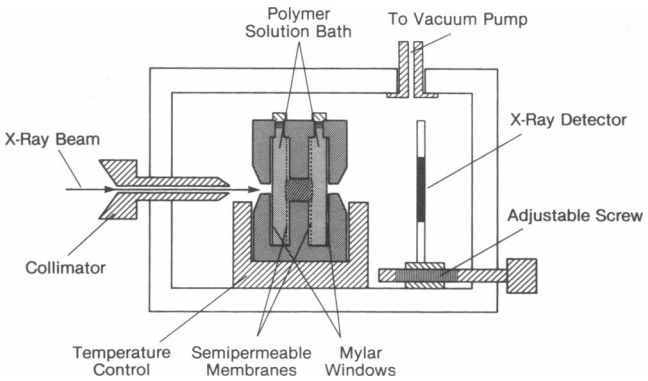

FIGURE 1 Schematic representation of osmotic stress force measurement method, as described in the text.

The complex is sufficiently stable under these salt conditions that no change in spacing is observed even after repeated cycling of a sample between high and low osmotic pressures. We have additionally compared spacings we measure with interhelical distances determined by Suwalsky and Traub (1977) for salmon sperm nuclei at 92% relative humidity (Fig. 3).

X-ray measurements

Distances between helices in DNA pellets equilibrated against PEG-salt solutions are determined by x-ray scattering. An Enraf-Nonius Service Corp. (Bohemia, NY) fixed anode Diffractis 601 x-ray generator equipped with a high power, fine focus, copper tube is used for these measurements. The camera was designed and built at the NIH (Mudd et al., 1987). The sample cells contain both the DNA pellet and ~100 μl of the bathing PEG-salt solution, sealed against evaporation, and temperature regulated. The camera chamber is evacuated to minimize air scattering. X-ray reflections from the DNA pellet are detected by film (DEF 5; Eastman-Kodak Co.). The very strong equatorial reflections can be measured either by hand or by a scanning densitometer (Podgornik et al., 1989) to give a Bragg spacing between helices. The 14.5 Å Bragg reflection from powdered bromobenzoic acid was used to calibrate the sample to film distance (~15 cm). Occasionally, DNA samples are exposed long enough to obtain higher order reflections to confirm hexagonal packing and to observe the 3.4 Å reflection characteristic of B-form DNA. The relation between the Bragg spacing, D_{Br}, and the actual distance between helices, D_{int}, for this packing is,

$$D_{int} = 2D_{Br}/\sqrt{3}. \quad (1)$$

Equatorial reflections are sharp and well defined for interaxial spacings < 30 Å. Most pellets give powder pattern ring reflections. It is not unusual, however, for a sample to give a strongly oriented scattering pattern. For the same ionic conditions and PEG osmotic pressure, interaxial spacings from these oriented samples are not different from powder pattern measurements. Interaxial spacings are reproducible to within ±0.2 Å for different samples equilibrated against the same PEG, salt conditions. The measurements reflect reversible thermodynamic equilibria. Interhelical spacings do not depend on the origin of initial DNA pellet, either a loosely packed 5% PEG phase-separated sample, a very tightly packed ethanol precipitate, or DNA assembled with a large excess of multivalent ion. Samples equilibrated against one set of PEG, salt, and polyvalent ion concentrations can be reequilibrated against another set and give the same spacing as a pellet directly equilibrated against the second set.

RESULTS

Force curves between attractive Co^{3+}-DNA helices

Much work has already been done by others characterizing salt conditions necessary for DNA precipitation by polyvalent ions (Gosule and Schellman, 1978; Wilson and Bloomfield, 1979; Widom and Baldwin, 1980, 1983). The assembly process can be conveniently monitored by changes in light scattering intensity or flow dichroism as large, random coiled helices collapse into compact, toroidal structures with a sufficient polyvalent ion concentration (e.g., Chattoraj et al., 1978; Allison et al., 1981). Observations pertinent to our experiments are that collapse occurs over a very narrow range of polyvalent ion concentration and that this critical concentration depends on bulk NaCl concentration (Wilson and Bloomfield, 1979; Widom and Baldwin, 1980, 1983). The minimum polyvalent ion concentration necessary for precipitation increases with increasing NaCl concentration. Given the strong ion-binding characteristics of DNA and the competition between Na^+ and polyvalent ions for binding (e.g., Manning, 1978; Record et al., 1978), the salt dependence of the critical polyvalent ion concentration has been interpreted as implying that a sufficient number of polyvalents must be bound to the surface to lower the charge density enough for precipitation.

The force curves shown in Fig. 2 illustrate the differences between the repulsive forces reported by us previously (Rau et al., 1984) and those between DNA helices that have spontaneously precipitated into hexag-

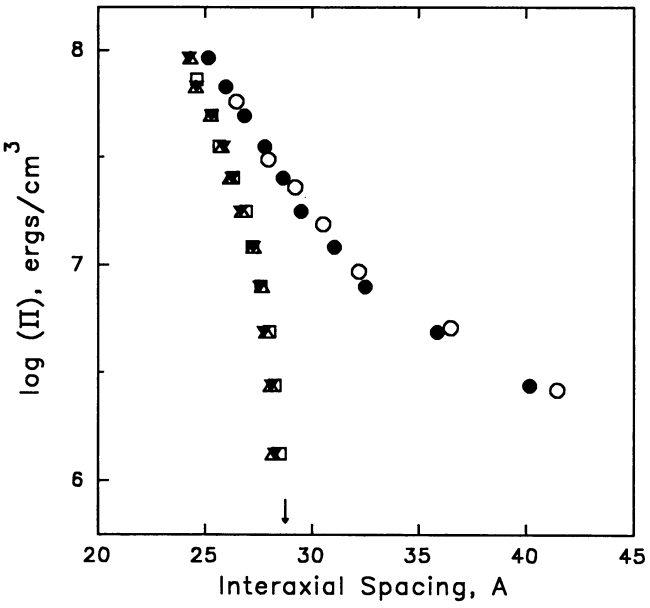

FIGURE 2 Comparison of intermolecular force curves ($\log_{10}$ of PEG osmotic pressure, Π, versus interhelical spacing, D_{int}) measured for helices spontaneously assembled with $Co(NH_3)_6Cl_3$ under a variety of solution ionic conditions and measured between helices that are repulsive at all distances in NaCl solutions, all at 20°C. 0.25M NaCl, 10 mM TrisCl (pH 7.5), 1 mM EDTA (○). 0.50M NaCl, 10 mM TrisCl, 1 mM EDTA (●). 1 mM $Co(NH_3)_6Cl_3$, 10 mM TrisCl (7.5) (□). 20 mM $Co(NH_3)_6Cl_3$, 0.25 M NaCl, 10 mM TrisCl (△). 100 mM $Co(NH_3)_6Cl_3$, 0.25 M NaCl, 10 mM TrisCl (▼). Note that force curve characteristics of both repulsion and net attraction are independent of salt concentration, but that the apparent exponential decay lengths of the two differ by a factor of ~2.

onal arrays after the addition of sufficient $Co(NH_3)_6Cl_3$. These curves relate measured interhelical spacing D_{int} to log of the osmotic stress (Π) exerted by PEG-salt solutions in equilibrium with the DNA lattices.

The rightmost curves show the forces in 0.25 and 0.5 M NaCl. We had previously observed for these purely repulsive forces that, at interaxial distances >30–35 Å, force magnitudes and slopes are ionic strength dependent and arise from fluctuation-enhanced electrostatic repulsion (Podgornik et al., 1989; Podgornik and Parsegian, 1990). At higher pressures and closer distances, we observe an exponentially growing force with an apparent ~3 Å decay length. Force magnitudes in this region do not depend on ionic strength, but are sensitive to the particular counterion bound on the DNA surface (Rau et al., 1984). The ~3 Å decay length is independent of both ionic strength and counterion species. We have characterized these forces as arising from repulsive water structuring between helices, repulsive "hydration" forces.

The other, leftmost, three curves in Fig. 2 are for DNA to which enough Co^{3+} is added to cause helices to assemble spontaneously into a hexagonal array. Two curves are with 20 and 100 mM trivalent Co^{3+} in 0.25 M NaCl, 10 mM TrisCl. The third curve is for DNA precipitated in 1 mM Co^{3+}, 10 mM Tris-Cl, without added NaCl.

The three curves superpose and show a common set of force characteristics. In the absence of applied stress, there is a stable, finite center-to-center separation of ~28.3, or 8.3 Å between surfaces. The base pair concentration at this spacing is ~1 M. Such a finite equilibrium separation implies a balance between attractive forces that bring the helices together from infinite separation and repulsive forces acting at very short distances.

The measured forces probe the characteristics of the close distance repulsive side of the energy well. With added osmotic pressure, we can bring the helices closer, down to 22 Å interaxial spacing at the highest pressure. The force characteristics observed here greatly restrict possible candidates for the close distance repulsion. The insensitivity of the equilibrium ($\Pi = 0$) spacing and observed forces to ionic strength and to added Co^{3+} argues strongly against a significant contribution from electrostatic double layer forces.

At higher pressures, away from the minimum in the energy well, the curve is accurately described by an exponentially increasing force with a 1.4 ± 0.1 Å decay length. The repulsive component of the net force is not the ~3 Å value characteristic of hydration repulsion found between DNA helices in NaCl only.

Force curves with other polyvalent ions

Several polyvalent counterions besides Co^{3+} cause DNA precipitation with finite equilibrium separation. Fig. 3 shows molecular force curves for four very different polyvalent cations, the highly basic oligopeptide salmon protamine, the alkyl triamine spermidine, $Co(NH_3)_6Cl_3$, and $Mn(ClO_4)_2$. In general, counterions that cause precipitation of DNA are charged +3 or more but there are several divalent transition metal ions, such as Mn^{2+}, that cause spontaneous assembly either at elevated temperatures or in conjunction with chaotropic coions (Rau and Parsegian, 1992; Knoll et al., 1989). Protamines are used to package DNA tightly in the sperm heads of many species. On average, protamines are ~20 amino acids long and contain ~70% arginine and lysine (e.g., Suau and Subirana, 1977; Herskovits and Brahms, 1976). At a constant NaCl concentration, there are significant differences in the critical concentrations of specific polyvalent ions necessary for precipitation. Approximately five-to-six times as much trivalent spermidine, for example, is required for assembly in 0.1 M NaCl than trivalent cobalt hexamine (Wilson and Bloomfield, 1979; Widom and Baldwin, 1980).

Equilibrium spacings at $\Pi = 0$, indicated by the

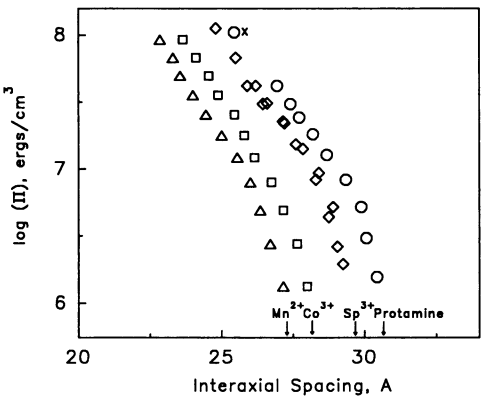

FIGURE 3 Comparison of intermolecular force curves measured between helices spontaneously assembled by a variety of 'condensing' cations, from polymeric protamine to divalent Mn^{2+}, at 20°. Salmon protamine, 10 mM TrisCl (pH 7.5) (○). Interhelical spacing at 92% relative humidity ($\log(\pi) = 8.04$) of salmon sperm heads (taken from Suwalsky and Traub, 1972) (x). 2 mM $SpermidineCl_3$, 10 mM NaCl, 10 mM TrisCl; and 10 mM $SpermidineCl_3$, 0.1 M NaCl, 10 mM TrisCl (◇). 5 mM $Co(NH_3)_6Cl_3$, 0.1 M NaCl, 10 mM TrisCl (△). 150 mM $Mn(ClO_4)_2$, 10 mM TrisCl (□). The arrows at the bottom of the figure give the equilibrium spacings between helices in the absence of externally applied osmotic pressure for protamine, spermidine, cobalt hexammine, and manganese. Salmon sperm nuclei at 100% relative humidity have an interhelical spacing of ~30.4 Å (Suwalsky and Traub, 1972). Note the similarity of force characteristics for all ions.

arrows in the figure, depend on the particular ion causing assembly. This has also been reported by Schellman and Parthasarathy (1984), who find D_{eq} = 29.4 Å for spermidine with calf thymus DNA and 28.2 Å for cobalt hexammine with chicken erythrocyte DNA. The magnitude of the repulsive part of the energy minimum, that is the force needed to push helices closer than the equilibrium spacing, also depends on polyvalent ion identity. At high pressures, however, all four curves are well characterized as exponentially increasing forces with decay lengths 1.3–1.5 Å, independent of counterion species.

These force characteristics are closely similar to the properties that led us to conclude that repulsive hydration forces dominate the forces between helices in univalent counterion solutions. Force magnitudes depend on counterion identity, but not concentration; exponential decay lengths are independent of both. The very striking difference from our previous observations is that the decay length associated with an attractive energy minimum is very close to half that for overall net hydration repulsion (1.4 ± 0.1 vs. 3 ± 0.3 Å).

Equilibrium spacings in mixed methanol water solutions

Wilson and Bloomfield (1979) have reported that divalent ions such as Mg^{2+} are sufficient to cause precipitation in 50:50 (vol/vol) methanol–water solutions. Additionally, much lower concentrations of polyvalent ions are required for spontaneous assembly than in water at the same ionic strength. Schellman and Parthasarathy (1984) have measured a 26.7 Å equilibrium spacing between DNA helices in $MgCl_2$ and 50% methanol. This very small separation together with the dependence of equilibrium spacings in water on the size of the polyvalent ion led Schellman and Parthasarathy to suggest that a tight counterion-DNA phosphate cross-bridging complex is formed between two helices.

We have extended these equilibrium spacing measurements to include other polyvalent ions in water–methanol mixtures. Fig. 4 shows the variation in equilibrium spacing for three ions, $Co(NH_3)_6^{3+}$, spermidine^{3+}, and Mg^{2+} in a series methanol–water mixtures. It is apparent that spacings are very sensitive to methanol concentration for all these ions. At 50% methanol, only little more than 1 Å separates the equilibrium spacings for all three ions, in spite of the difference in sizes. Spacings decrease by more than 3 Å for both Co^{3+} and Sp^{3+} between 0 and 50% methanol solutions. Even more dramatically, the equilibrium spacing with Mg^{2+} precipitation decreases by ~6.5 Å between 25 and 50% methanol in 20 mM $MgCl_2$, from 32.5 to 26 Å. Equilibrium spacings are not simply related to counterion size.

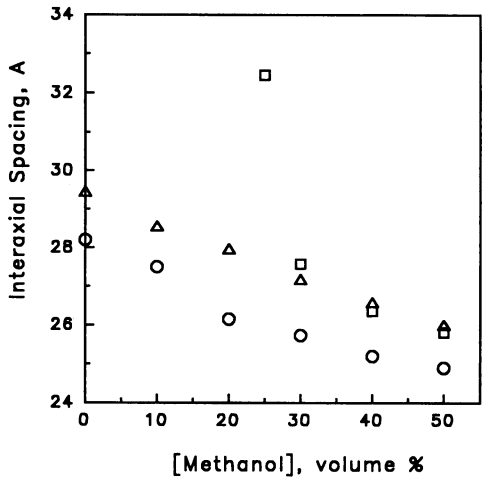

FIGURE 4 Dependence of the equilibrium spacing ($\Pi = 0$) on methanol volume fraction in mixed water/methanol solvents for three ions at 20°. 20 mM $MgCl_2$, 10 mM TrisCl (□). 20 mM SpermidineCl$_3$, 10 mM TrisCl (△). 2 mM $Co(NH_3)_6Cl_3$, 10 mM TrisCl (○). Equilibrium spacings decrease montonically with increased methanol concentration for all three ions. Spontaneous precipitation of DNA with 20 mM Mg^{2+} requires at least 25% methanol.

Force curves with subcritical Co^{3+} concentrations

Critical Co^{3+} concentrations effecting DNA collapse are most commonly determined by monitoring DNA aggregate size by light scattering while titrating with Co^{3+} in aqueous salt solutions. The same type of experiment can be done monitoring interhelical spacing at constant applied osmotic pressure while titrating with Co^{3+}. Fig. 5 shows these results in 0.25 M NaCl. Interhelical distances initially decrease smoothly with increasing Co^{3+} concentration. Across a fairly narrow range of trivalent concentrations there is apparent a sudden and abrupt decrease in spacing. Interhelical distances decrease very slowly after this. The spacing after the abrupt transition is characteristic of that seen for DNA spontaneously precipitated by Co^{3+} from aqueous solution, shown by the circles in the figure. The trivalent concentration at which the transition occurs depends on the osmotic pressure applied. At greater external pressures, transitions are apparent at lower Co^{3+} concentrations.

The sudden decrease in spacing observed corresponds to abrupt transition from net repulsive to net attractive helices, in much the same way as helices in aqueous salt solutions in the absence of an external pressure assemble from a extended random coil conformation into a compact structure over a narrow range in Co^{3+} concentrations.

Fig. 6 shows an alternate representation of the interplay among Co^{3+} concentration, osmotic pressure, and

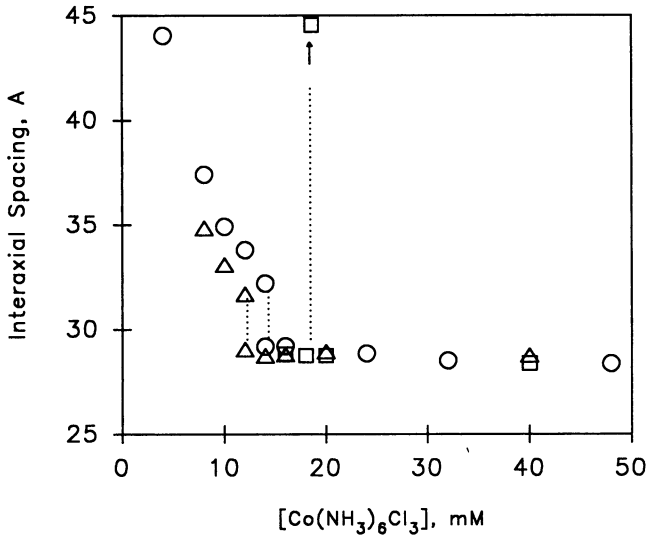

FIGURE 5 Interhelical spacings versus cobalt hexammine concentration for DNA held under gentle, but constant, osmotic stress in 0.25 M NaCl, 10 mM TrisCl, at 20°. Π = 0 (□). log(Π) = 5.95 (○). log(Π) = 6.15 (△). The abrupt change in spacing occurs within a concentration span of ~0.25 mM. The transition in the absence of applied osmotic pressure occurs at 17 mM Co^{3+} as a sudden collapse from dilute solution to an approximate 28 Å spacing, illustrated by the arrow.

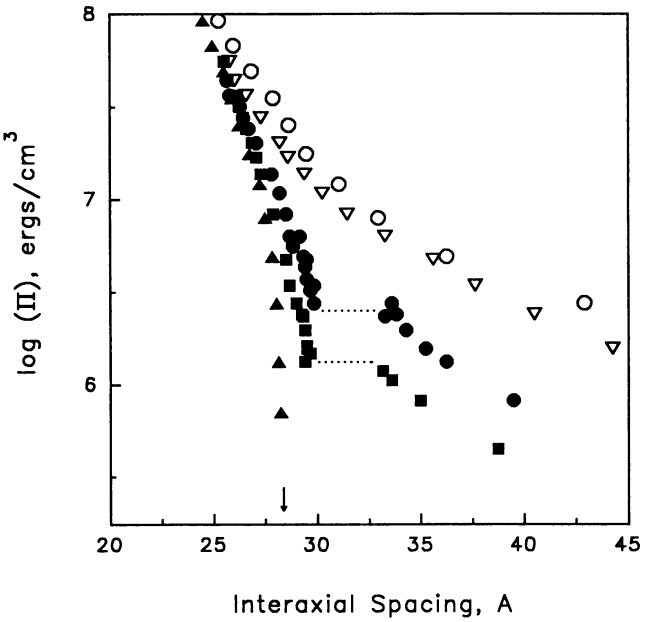

FIGURE 6 Intermolecular force curves for a series of cobalt hexammine concentrations in 0.25 M NaCl, 10 mM TrisCl (pH 7.5), at 20°. Spontaneous precipitation occurs at 17 mM Co^{3+} at this ionic strength. 0 mM $Co(NH_3)_6Cl_3$ (○). 2 mM (▽). 8 mM (●). 12 mM (■). 20 mM (▲). Abrupt transitions from one kind of force curve to another indistinguishable from the 20 mM data are clearly apparent for the 8 and 12 mM data.

force characteristics. Complete force curves are shown for five Co^{3+} concentrations in 0.25 M NaCl, at 20°C. The 0 and 20 mM Co^{3+} added curves represent the two extremes in forces: the first showing net repulsion at all distances with an ~3 Å exponential decay length at high pressures; and the second beginning from an equilibrium, minimum energy, spacing then, closer in, showing the repulsive side of the energy well that is characteristic of net attraction with its ~1.4 Å decay length.

The force curve with 2 mM added Co^{3+} is only slightly different from the no-Co^{3+} curve. The two curves are closely parallel. Force curves in 8 and 12 mM Co^{3+}, in contrast, show clear transitions. At low pressures and large spacings (>30–35 Å), forces resemble the NaCl-only curve with exponential decay lengths 3–8 Å. Force magnitudes depend strongly on bulk Co^{3+} concentration. At a critical osmotic pressure, dependent on trivalent concentration, an abrupt decrease in the interhelical spacing is observed. After these transitions, force curves then closely superimpose with 20 mM Co^{3+} data. Transitions are sharp, occurring within an ~2% change in log (Π). Transition pressures increase with decreasing bulk trivalent concentration.

These curves are fully reversible. DNA samples equilibrated against PEG solutions at high osmotic pressures after the apparent transition can be reequilibrated against low osmotic pressure PEG solutions and show no hysteresis.

These transitions are clearly from forces that are characteristic of net repulsion to a curve that is indistinguishable from the spontaneously Co^{3+}-precipitated data. The work done by the osmotic pressure on the helices perturbs the equilibrium between repulsion and attraction. This perturbation is not seen as a gradual shift of the data between the two extremes, but rather in a sudden, discrete jump from one curve to the other. Osmotic stress does not effect a transition with Co^{3+} concentrations less than ~2–4 mM. The effect of osmotic pressure appears to be all-or-none. Either sufficient work is done to cause the transition or little effect on the force is observed (approximately parallel curves).

DISCUSSION

We have previously characterized forces between DNA helices for several different uni- and divalent cations (Rau et al., 1984; Parsegian et al., 1985; Parsegian et al., 1987). Under these salt conditions, DNA helices repel at all separations. At interaxial distances <30–35 Å (sur-

face separations < 10–15 Å), exponentially varying repulsion decays with a characteristic length of ~3 Å. The decay length and magnitude of this repulsion are surprisingly insensitive to ionic strength or to the type of ion in the suspending medium. Only the coefficient of this force is changed in the presence of different cations.

Then, at greater separations, repulsion is sensitive to ionic strength. But, the decay rate is approximately one-half that expected from Debye Huckel double layer theory. By direct measurement both of the intermolecular force versus separation as well as of the change in disorder of the flexible DNA molecules, it was found that at these larger separations there is steric undulatory enhancement of electrostatic double layer or of hydration forces, a coupling between thermal disorder of molecular bending with the intermolecular repulsion that suppresses that bending (Podgornik et al., 1989; Podgornik and Parsegian, 1990).

In contrast, here DNA molecules "condensed" by polyvalent cations assemble into well defined lattices with interaxial distances much greater than the diameter of double helices. These distances imply the action of long range attraction acting to create energy minima at 8 to 12 Å separation between molecular surfaces. Direct measurement of the forces needed to push molecules together from these spontaneously assumed positions reveal an exponential repulsion of 1.3 to 1.5 Å decay length. This is one-half the value seen in cases of pure repulsion. This ~1.4 Å decay is stubbornly insensitive to ionic strength and even to the identity of condensing species. Only the spontaneous separations of collapsed structures change with the identity of the condensing agent. These data fit neither of the previously imagined mechanisms for counterion condensation, and lead us to recognize the possibility of attractive forces based on solvent restructuring of the water between neighboring double helices.

At first thought, polyvalent cations might be acting indirectly by allowing molecules to come close simply by screening electrostatic double layer (esdl) potentials enough to allow van der Waals attraction to pull molecules together. This is the kind of balance expected in classical colloid theory. This traditional view is rendered invalid by two qualitative features of the measured forces.

First, the ~1.4 Å decay length exponential repulsion, between molecules forced together from equilibrium separation at a distance, is affected neither by the valence nor the ionic strength of the condensing agent; it bears no relation to the predictions of electrostatic double layer theory.

Second, added NaCl, which if anything should further screen electrostatic double layer repulsion, causes the condensed pellet suddenly to come apart. The concentration of polyvalent ion necessary for assembly increases with increasing NaCl concentration (Wilson and Bloomfield, 1979; Widom and Baldwin, 1980, 1983).

Our data supports a direct role for bound polyvalent ions in the precipitation of DNA. One extreme would be that the various agents can form direct cross-bridge links between neighboring molecules. Indeed, the dependence of the equilibrium spacing on polyvalent ion species seemed to imply that this distance is determined by the size of the polyvalent ion through the formation of tight complexes between a phosphate on one helix, the polyvalent ion, and a phosphate on an apposing helix.

In support of a tight bridging complex, Schellman and Parthasarathy (1984) measured the equilibrium spacings of Mg^{2+}-precipitated DNA in 50:50 methanol–water solution. The 25–26 Å interaxial spacing observed fit well with a series of spacings seen for DNA precipitated with larger polyvalents in pure water. Ion size seemed to correlate well with spacing. Now, having measured interaxial spacings between DNA helices precipitated in a range of methanol:water ratios and having measured forces for DNA precipitated by several kinds of ions, we find that the correlation between spacing and ion size no longer holds.

First, it is difficult to rationalize the 32 Å spacing observed with Mg^{2+} in 25% methanol as a well structured Mg^{2+}-PO_4^- complex. This spacing is vastly bigger than those seen with Sp^{3+} or Co^{3+} at the same methanol concentration. The earlier size-spacing correlation works only if the DNA is in solutions of very different methanol concentration.

Second, it is even more difficult to see how a cross-linking or tight-complex mechanism can lead to a common 1.4 Å exponential repulsion for DNA condensed by agents as different as Mn^{2+}, $Co(NH_3)_6^{3+}$, Sp^{3+}, and polymeric protamine. The "sponginess" of a tightly bridged complex should depend on the identity of the counterion.

Osmotic stress mediated transitions

The sensitivity of force magnitudes at low pressures to $Co(NH_3)_6^{3+}$ concentration seen in Fig. 6 results from the sensitivity of hydration forces to the type of counterion bound to the DNA surface. Just as we found previously (Rau and Parsegian, 1984) that force magnitudes, but not the exponential force characteristics, are dependent on the particular univalent or divalent cation in solution, so also will the force magnitude be dependent on the relative fraction of bound Na^+ and $Co(NH_3)_6^{3+}$ in mixed uni- and trivalent solution. This observed sensitivity also implies a dependence of Co^{3+} binding (or Co^{3+}/Na^+ exchange) on interhelical spacing. Similarly, the insensitivity of molecular force curves for spontaneously precip-

itated DNA to bulk Co^{3+} concentration and the superposition of force curves with subcritical Co^{3+} at high pressures with the curves for spontaneously precipitated DNA implies a limiting or saturating binding of trivalent ion to DNA. The measurement of forces by the osmotic stress technique under well defined solution conditions allows one to apply fundamental thermodynamic relationships to determine the changes occurring with Co^{3+} binding occurring.

The osmotic stress experiment is thermodynamically equivalent to an experiment in which a piston with a semipermeable membrane applies a mechanical pressure on the DNA phase. The membrane separates the DNA containing phase from a reservoir salt solution (without PEG) of fixed ion and water activity. The mechanical pressure is equivalent to the osmotic pressure of the PEG in the stress experiment. We assume that the ion and water activities are the same in the reference reservoir and in the DNA phase and that the exchangeable volume between the two is entirely from water, i.e., that the volume of DNA itself is constant and that the volume of exchanging ions is very small compared with water. A more complete description of the thermodynamic connection between the osmotic stress and mechanical pressure experiments is given in Leikin et al. (1991).

The osmotic stress versus interaxial separation relations of Fig. 6 are thermodynamic measures of the state functions that govern molecule force and assembly. These curves indicate the change in the DNA containing phase free energy dG with experimental variables, specifically osmotic stress Π and Co^{3+} chemical potential μ_{Co}. With each of these variables there is a corresponding conjugate variable, the volume of the DNA phase, V, for the osmotic pressure and the number of bound Co^{3+}, or, more precisely, the number of ions associated with the DNA phase, n_{Co}, for the trivalent ion chemical potential. If all other experimental variables, temperature, NaCl activity, etc., are held constant, then the change in system free energy can be written

$$dG = V d\Pi - n_{Co} d\mu_{Co}, \tag{2}$$

where we recognize that $\partial G/\partial \Pi = V$ and $\partial G/\partial \mu_{Co} = -n_{Co}$. Because G is a state function we can immediately write down a Maxwell relation,

$$(\partial n_{Co}/\partial \Pi)_{\mu} = -(\partial V/\partial \mu_{Co})_{\Pi}. \tag{3}$$

The change in number of Co^{3+} ions associated with the DNA phase can be calculated from,

$$\Delta n_{Co} = \int \partial n_{Co} = -\int \frac{\partial V}{\partial \mu_{Co}} d\Pi = -\frac{\partial}{\partial \mu_{Co}} \int V d\Pi. \tag{4}$$

Using the bulk Co^{3+} concentration-independent force curve of spontaneously precipitated DNA as a common reference state, the change in the number of bound Co^{3+} for those force curves with subcritical Co^{3+} concentrations that show an abrupt change in spacing and merge with the spontaneously precipitated force curve is given by,

$$\Delta n_{Co} = -\frac{d}{d\mu_{Co}} \int \Big(V([Co]) - V^* \Big) d\Pi, \tag{5}$$

where $V([Co])$ is the water volume associated with a particular osmotic pressure and subcritical cobalt concentration and V^* is the corresponding volume for spontaneously precipitated DNA. The integral is taken from $\Pi = 0$ to the pressure at which the two curves superimpose. Over this bounded region, the integral can be transformed to,

$$\Delta n_{Co} = \frac{d}{d\mu_{Co}} \int \Big(\Pi([Co]) - \Pi^* \Big) dV. \tag{6}$$

The integral in this equation simply represents the difference in total Π-V work done between pushing DNA helices at a subcritical Co^{3+} concentration from large spacing through the abrupt transition to the limiting force curve at high pressures and pushing DNA helices spontaneously precipitated with Co^{3+} from the equilibrium separation to the same endpoint. This work difference is illustrated in Fig. 7 for 12 mM $Co(NH_3)_6Cl_3$. The dependence of this work difference on cobalt chemical potential (here assumed as $kT \ln([Co^{3+}])$ at these salt concentrations) directly gives changes in trivalent ion binding.

Fig. 8 shows this net Π-V work as a function of the bulk Co^{3+} concentration. The minimal Co^{3+} concentration (17 mM) necessary for spontaneous precipitation in the absence of an externally applied osmotic pressure ($\Pi = 0$) is included in this figure as the point that corresponds to a Π-V work of 0 kT. The data can be well described by a quadratic in ln $[Co^{3+}]$ (in mM concentration) of the form,

$$W_{total}([Co^{3+}]) = 0.955 - 0.484 \ln [Co^{3+}] + 0.052(\ln [Co^{3+}])^2. \tag{7}$$

This equation is consistent with the result of Fig. 6 that below a certain Co^{3+} concentration no abrupt transition is observed. This Π-V work represents a repulsive energy or stress on the system that can be relieved by binding extra Co^{3+}. If enough extra trivalent ion is bound, the DNA assembly will undergo a transition resulting in a force curve characteristic of the spontaneously precipitated DNA. The work shown in Fig. 8 gives the amount of stress necessary for this

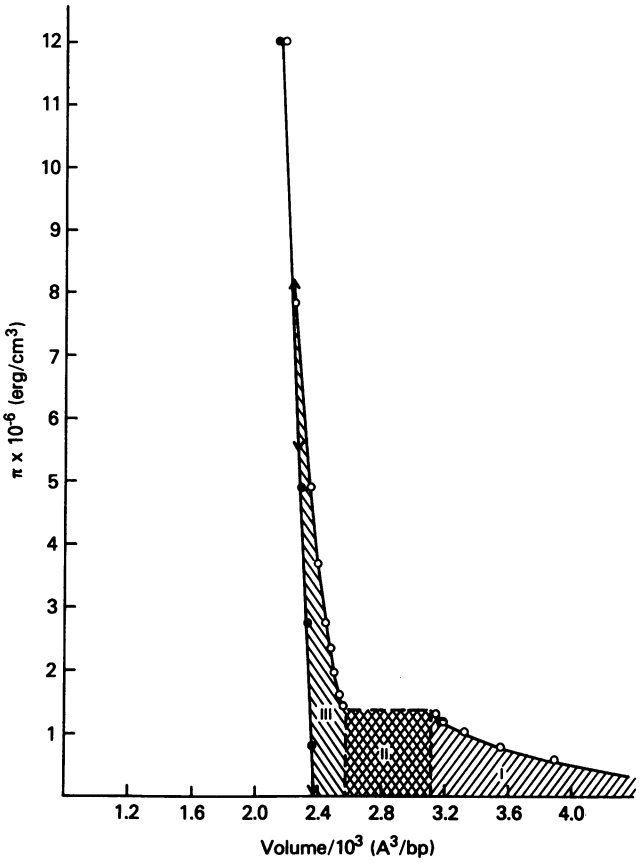

FIGURE 7 Pressure–volume work characterizing the transition from repulsion at a subcritical cobalt concentration to the spontaneously precipitated force curve is illustrated. 12 mM $Co(NH_3)_6Cl_3$, 0.25 M NaCl, 10 mM TrisCl (○). 20 mM $Co(NH_3)_6Cl_3$, 0.25 M NaCl, 10 mM TrisCl (●). The shaded area shows the difference in Π-V work between the 12 and 20 mM Co^{3+} data that superimpose at high pressures. Numerical calculations for regions I and III are most conveniently done by fitting force data with exponential splines and integrating piece-wise. For hexagonally packed helices, the relation between V (per base pair) and the interaxial spacing D gives $dV = \sqrt{3}\, l\, D\, dD$, where l is the distance along the helix between base pairs (3.4 Å). At the transition pressure (region II), the work in compacting the array from a spacing D_2 to D_1 is simply $\sqrt{3}\, \Pi_t\, l\, (D_2^2 - D_1^2)/2$. For distances beyond 50 Å, we extrapolate the force curve observed at low pressures. We assume that the difference in work in simply extrapolating the low pressure data and in actually concentrating random coils from dilute solution to a 50 Å separation is small compared to the total work. The extrapolated work contributes less than about 10% to the total.

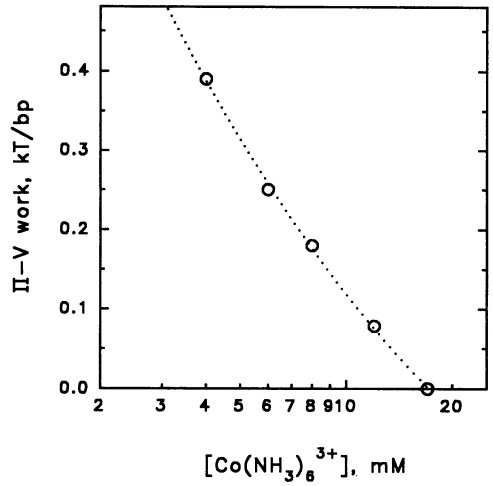

FIGURE 8 The dependence of the total Π-V work (expressed in units of kT/base pair) done on helices to effect the transition on bulk cobalt hexammine concentration is shown. The line through the points is the best quadratic fit to the data.

transition as a function of trivalent concentration. Extrapolating back to 2 mM Co^{3+}, a predicted 0.65 kT/bp of work would be necessary. The difference between the 2 and 20 mM Co^{3+} force curves, however, only allows a maximum of 0.60 kT/bp. There is not sufficient Π-V work available compared with stress required for the transition.

From the quadratic fit to the data in Fig. 8 and Eq. 6, we have for the number of extra Co^{3+} ion bound per base pair,

$$\Delta n_{Co} = n_f - n_i = 0.484 - 0.104 \ln [Co^{3+}]. \quad (8)$$

We infer a substantial change in cobalt binding between isolated helices and the collapsed state within this concentration range. At 4 mM $Co(NH_3)_6^{3+}$, $\Delta n_{Co} = +0.34$/bp; while even at the 17 mM concentration that is sufficient for spontaneous assembly, $\Delta n_{Co} = 0.20$/bp.

This change in number bound or associated with the DNA is simply the difference in the number bound initially, n_i, with widely separated helices and finally, n_f, after force curves superimpose with the data from spontaneously precipitated DNA. The insensitivity of the limiting force curve to bulk trivalent concentration argues that this final number bound is at least fairly constant. Eq. 8, therefore, essentially describes a Co^{3+} binding curve that can be compared with binding data obtained by more traditional methods.

Plum and Bloomfield (1988) have measured Co^{3+} binding by equilibrium dialysis at salt concentrations somewhat lower than our 0.25 M NaCl, fitting their data to the binding formalism of McGhee and von Hippel (1974). We use the Plum and Bloomfield expression for the dependence of the binding constant on ln [NaCl], and calculate the expected Co^{3+} binding in 0.25 M NaCl. This curve, showing the number of bound Co^{3+}/bp as a function of ln [Co^{3+}], is the solid line in Fig. 9. The range of trivalent ion concentrations over which we calculate a binding curve for Co^{3+} from transitions in force curves is indicated by the brackets. Within this concentration

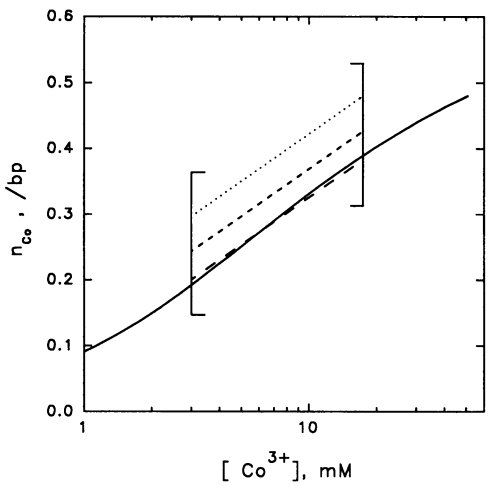

FIGURE 9 Comparison of $Co(NH_3)_6^{3+}$-DNA binding curves extracted from the dependence of the Π-V work on bulk cobalt hexammine concentration with the binding extracted from the equilibrium dialysis data of Plum and Bloomfield (1988). The brackets indicate the concentration range of cobalt hexammine over which osmotic pressure induced transitions in force curves can be observed and binding extracted from the work. The binding curve generated from the fitting parameters of Plum and Bloomfield extrapolated to 0.25 M NaCl (———). The binding curve extracted from the Π-V work with a maximal binding of 0.66 Co^{3+}/bp (complete charge neutralization) after the transition (. . . . .). Π-V work derived binding with n_{Co} = 0.61 Co^{3+}/bp, the maximal +3 ion binding within the Manning counterion condensation formalism for isolated helices (- - -). Extracted Co^{3+} binding with n_{Co} = 0.58, which best fits the Plum and Bloomfield curve (— —).

range, the binding curve generated from the Plum and Bloomfield data can be described by a straight line of the form,

$$n_i(/\text{bp}) = 0.070 + 0.116 \ln [Co^{3+}]. \quad (9)$$

Comparing this with the binding equation extracted from the osmotic stress induced transitions, Eq. 8, we see that the ln $[Co^{3+}]$ coefficients differ by only ~10%. The constant term of the osmotic stress derived binding equation depends on the final number of Co^{3+} bound. We can make several estimates of this for comparison with the binding curve generated from the results of Plum and Bloomfield. The dotted and dashed lines in Fig. 9 show the osmotic stress extracted binding curves for complete charge neutralization by bound Co^{3+} (n_f = 0.67 Co^{3+}/bp) and for the maximal charge neutralization by +3 ions within the Manning counterion condensation theory for isolated helices (Manning, 1978) (n_f = 0.61 Co^{3+}/bp, 92% charge neutralization), respectively. These maximal estimates give curves that show binding only 20 to 40% higher than the extrapolated experimental curve over the bracketed range of Co^{3+} concentrations. Alternatively, the value of n_f that gives the best fit between the two sets of data is 0.58 Co^{3+}/bp.

Within experimental error, Co^{3+} binding at 0.25 M NaCl extracted from the osmotic stress induced transition data is in very reasonable agreement with the Plum and Bloomfield experimental estimates of binding, provided that attractive helices are close to completely saturated with bound Co^{3+} (n_f ~ 0.6).

We can now also estimate the depth of the energy minimum for spontaneously precipitated Co^{3+}-DNA. Eq. 2 emphasizes the trade-off between Π-V work and Co^{3+} binding. Combining Eqs. 7 and 8, we can extrapolate the Π-V work to Δn_{Co} = 0 and eliminate the energetics of extra Co^{3+} binding from the force balance. The extrapolated Π-V work is ~ −0.17 kT/bp (or −100 cal/mol bp). This corresponds to the work done by DNA helices in assembling from dilute solution to the 28 Å equilibrium spacing at sufficiently high cobalt concentration such that there is no change in Co^{3+} binding during the precipitation. This is the depth of the attractive energy minimum.

Could this energy minimum magnitude be accounted for by attractive van der Waals interactions as suggested by Bloomfield et al. (1980)? If we assume a large value for the Hamaker coefficient of DNA, 10^{-13} ergs, then an overestimate of the magnitude of the van der Waals attraction alone can be calculated for a hexagonal array of helices from the pairwise interaction formulas given by Brenner and McQuarrie (1973) for cylinders. For a 28 Å spacing and a 10 Å DNA radius, E_{vdW} = −0.025 kT/bp. This pure attractive energy which ignores any mitigating electrostatic or hydration repulsion is itself almost an order of magnitude smaller than the net attractive energy estimated above.

Attractive hydration forces can account for experimental observations

The data presented here eliminates several classes of interactions from consideration as important in the precipitation of DNA by multivalent ions. Classical van der Waals interactions are too small. The insensitivity of intermolecular force curves to bulk ionic strength means that double layer forces are not significant. We have already shown that our observations are inconsistent with a tight, hard sphere ion bridging of helices. What else might be going on? Although other types of interactions might be possible, perhaps unscreened attractive coulombic forces between helices with bound multivalent cations coupled with some sort of repulsive interaction, the dominance of repulsive hydration forces at close separation between DNA helices in solutions of uni- and divalent cations leads us first to explore

alternate hydration force schemes, in particular attractive hydration forces. The major difference between repulsive forces in NaCl, for example, and the residual repulsive force seen with multivalent ion assembled DNA is the factor of two change in exponential decay lengths. We have previously argued that attractive hydration forces are important for the forces between lipid bilayers (Rand et al., 1988; Kornyshev and Leikin, 1989) and have shown that this factor of two is a natural consequence of attractive hydration interactions.

The hydration force formalism developed by Marcelja and co-workers (e.g., Marcelja and Radic, 1976; Gruen et al., 1983) assumes that a hydrating surface perturbs in some way the water in contact with that surface. This perturbation is propagated through water–water interactions into the bulk solution. The decay length for the propagation is taken as ~3 Å to connect with experiment. Repulsive hydration forces result from a symmetric overlap of perturbed hydration atmospheres as two surfaces approach. It is convenient for us to picture the perturbation as a polarization of water bound to the surface. The propagation of this structuring perturbation into the solution is then due to the hydrogen bonding of this water in successive layers. In a simple-minded way, when two surfaces that polarize water in the same way approach, the overlapping perturbed water polarizations disrupt the hydrogen bonding network water prefers. Analogously, if two surfaces with complementary water structures (the surfaces polarize or structure water in opposite directions) approach, then a hydrogen bonding network from one surface to the other is reinforced (e.g., see Rand et al., 1988). Attractive hydration forces result.

Real surfaces are not so homogeneous. Water is not structured the same way on all parts of the surface. The various chemical groups on a real polymer will orient water differently. It is possible that two approaching surfaces have some apposing patches that are attractive and others that are repulsive. With Co^{3+} precipitated DNA, for example, apposing attractive patches could be a bound Ca^{3+} on one helix opposite a phosphate group on the other. Within the linear approximation used by Marcelja and Radic (1976), the net force between surfaces is just the sum of the two contributions.

For cylindrical geometry, the hydration free energy per base pair from pushing purely repulsive surfaces from infinite separation to a spacing D and the osmotic pressure at D are,

$$\Delta G_{hyd}(D) = \frac{2\pi l\lambda^2}{K_0(a/\lambda)} \frac{P_r^2 K_0(D/2\lambda)}{(K_0(a/\lambda)I_0(D/2\lambda) - K_0(D/2\lambda)I_0(a/\lambda))} \quad (10)$$

$$\Pi(D) = (2\lambda/D)^2 \left[\frac{P_r^2}{(K_0(a/\lambda)I_0(D/2\lambda) - K_0(D/2\lambda)I_0(a/\lambda))^2}\right], \quad (11)$$

where P_r^2 is a measure of the strength of the repulsive water structuring on the two surfaces; l, the distance along the helix between base pairs (3.4 Å for B-form DNA); a, the radius of the DNA cylinder (10 Å), λ the exponential decay length for the propagation of the water structuring; and the I and K functions are modified Bessel functions.

The corresponding free energy difference and osmotic pressure for surfaces with both attractive and repulsive apposing patches are given by,

$$\Delta G_{hyd}(D) = \frac{2\pi l\lambda^2}{K_0(a/\lambda)} \left[\frac{P_r^2 K_0(D/2\lambda)}{(K_0(a/\lambda)I_0(D/2\lambda) - K_0(D/2\lambda)I_0(a/\lambda))} - \frac{P_a^2 K_1(D/2\lambda)}{(K_1(D/2\lambda)I_0(a/\lambda) + K_0(a/\lambda)I_1(D/2\lambda))}\right] \quad (12)$$

$$\Pi(D) = (2\lambda/D)^2 \left[\frac{P_r^2}{(K_0(a/\lambda)I_0(D/2\lambda) - K_0(D/2\lambda)I_0(a/\lambda))^2} - \frac{P_a^2}{(K_1(D/2\lambda)I_0(a/\lambda) + K_0(a/\lambda)I_1(D/2\lambda))^2}\right], \quad (13)$$

where P_a^2 is a measure of the magnitude of the surface hydration perturbation that results in attraction. If $P_a^2 > P_r^2$, there is predicted an energy minimum at some finite cylinder separation, D_{eq}. At this spacing, the ratio of the perturbation magnitudes for the attractive and repulsive patches is given by,

$$\frac{P_a^2}{P_r^2} = \left[\frac{K_1(D_{eq}/2\lambda)I_0(a/\lambda) + K_0(a/\lambda)I_1(D_{eq}/2\lambda)}{K_0(a/\lambda)I_0(D_{eq}/2\lambda) - K_0(D_{eq}/2\lambda)I_0(a/\lambda)}\right]^2. \quad (14)$$

At large separations, the modified Bessel functions can be approximated by exponentials. Retaining only the two lowest order exponential terms, we have for Eq. 13,

$$\Pi(D) = -\frac{4a(P_a^2 - P_r^2)}{D} e^{-(D-2a)/\lambda} + \frac{8a(P_a^2 + P_r^2)}{D} e^{-2(D-2a)/\lambda}. \quad (15)$$

The first term on the right hand side describes the attractive force approaching the energy well from larger separations. It is exponential with decay length λ. The second term dominates the force for pushing helices closer than the equilibrium separation, the residual repulsive force. Again, this is an exponentially varying force but with half the decay length, $\lambda/2$, of the attractive term. This second-order term can be considered an image charge repulsion (Kornyshev and Leikin, 1989), a

change in solvation energy due to the steric exclusion of water by neighboring helices.

The magnitude of the attractive hydration force component is associated with the order parameter P_a^2, which is a measure of the solvent organizing ability of the interacting surfaces. The strength of attractive forces mediated by bound polyvalent ions will depend on the ability of the polyvalent to bind and organize water in its vicinity. The qualitative correlation of D_{eq} with ion size for trivalents might rationalized in terms of differences in water organizing power due to ion size. The difference in D_{eq} between Co^{3+} and Mg^{2+} at 25% methanol might be due to a difference in water structuring caused by the charge difference.

Within this theoretical framework, the equilibrium separation and the magnitude and exponential characteristics of the residual repulsive force are sufficient to determine all parameters in equation (13). Fig. 10 shows the best fit to the force data in 20 mM Co^{3+}. The parameters used in this fit are: $P_a^2 = 6.2 \times 10^7$ ergs/cm^3, $P_r^2 = 4.4 \times 10^7$ ergs/cm^3, and $\lambda = 4.5$ Å. With this mix of parameters, Eq. 12 gives an energy minimum at the 28 Å equilibrium separation of -0.15 kT/bp, in close agreement with the experimentally estimated depth (-0.17 kT/bp).

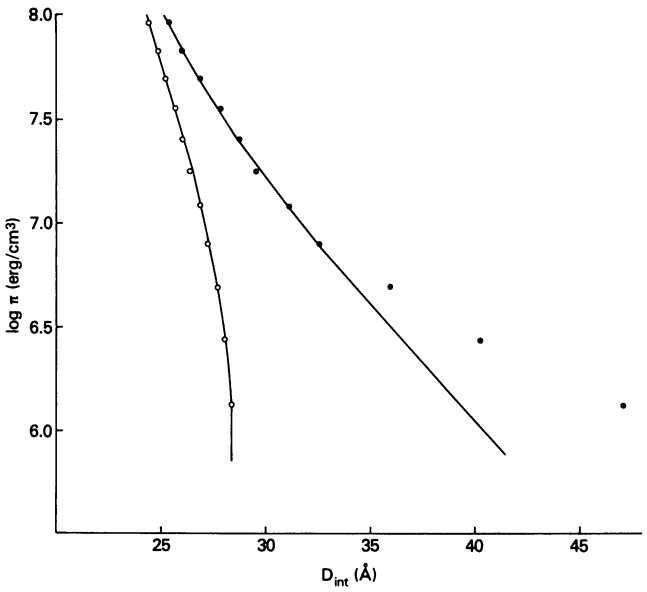

FIGURE 10 Best fits of experimental molecular force data at close separation for both net attractive and repulsive interactions to the theoretical expressions for hydration are shown. 0.5 M NaCl, 10 mM TrisCl, 1 mM EDTA. The solid line through the data is calculated from Eq. 11 with $P_r^2 = 4.3 \times 10^7$ ergs/cm^3 and $\lambda = 4.5$ Å (●). 20 mM $Co(NH_3)_6Cl_3$, 0.25 M NaCl, 10 mM TrisCl. The solid line through the data is calculated from Eq. 13 with the same decay length, $\lambda = 4.5$ Å, $P_a^2 = 6.2 \times 10^7$ ergs/cm^3, and $P_r^2 = 4.4 \times 10^7$ ergs/cm^3 (○).

The intrinsic decay length that best fits the data is some 50% larger than the 3 Å length observed directly in repulsive force data. This is strictly a consequence of the cylindrical geometry, Bessel functions do not reduce to simple exponentials. The same planar 4.5 Å decay length can also be used to fit the purely repulsive, 0.5 M NaCl force data, with only a P_r^2 parameter to fit the magnitude using Eq. 11. As seen in Fig. 10, there is also very good agreement between theory and experiment at high pressures. At lower pressures, fluctuation-enhanced double layer forces (Podgornik et al., 1989; Podgornik and Parsegian, 1990) make an additional contribution to the overall force, not included in Eq. 11. An intrinsic decay length for planar geometry of 4.5 Å results in a force curve that has an apparent 3 Å decay length for cylindrical geometry.

Consideration of hydration forces alone can quantitatively account for the molecular forces observed with counterion condensed DNA. The good fits shown in Fig. 10 between theory and experiment and the close agreement between the experimentally estimated and calculated energy minimum magnitudes underscores our conclusion that both the 3 and 1.5 Å decay length forces are manifestations of the same underlying force, the interaction of surfaces through perturbed water structuring.

While a net attractive energy of 100 cal/mol bp is not a large interaction energy, it is some 10–100 times larger than van der Waals attraction or double layer repulsion at these salt concentrations. It is easily sufficient to precipitate stiff DNA helices. Many base pairs contribute to the attraction without a proportionate loss of configurational entropy (e.g., Post and Zimm, 1979). The small net attractive energy is reflected in the large equilibrium separation of helices ($\sim$8 Å from surface to surface), compared with the apparent 3 Å decay length. The best fitting P_a^2 and P_r^2 parameters indicate that attraction is only slightly larger than repulsion. What happens if this remaining repulsion were turned into attraction, i.e., the water structuring on the two apposing surfaces is totally complementary with $P_{att}^2 = P_a^2 + P_r^2$, and $P_{rep}^2 = 0$? From Eq. 12, helices would approach touching, with no intervening water. The attractive energy expected would be about 3 kT/bp (2 Kcal/mol bp). This is a significant interaction energy. It also illustrates an inherent property of mixed attractive and repulsive hydration forces. Interaction energies show the specificity that is characteristic of many biological processes. Small changes in the structure of interacting

surfaces can cause large changes in the interaction energy.

For all its frustrating noncommittal to any physical model, the order parameter formalism does have the remarkable property of capturing the essential spirit of all second order perturbation theories. The relevant equations for scalar parameters are completely isomorphous to the Debye Huckel theory of weak electrostatic double layer potentials, where the role of order parameter is played by the electric field. The boundary conditions used by Marcelja and Radic (1976) are equivalent to constant charge surfaces, while those of Cevc et al. (1982) to constant potential. In some ways the attraction inferred from this model, sites of "positive" polarization due to adsorption of polyvalent cations opposite "negatively" polarized sites of unbound fixed phosphates, is a kind of charge pairing or salt bridge. But the physical mechanism apparent in the force law must differ from the Coulombic interaction in a continuum dielectric medium. Real solvent must be restructured in quite a different way.

Received for publication 3 May 1991 and in final form 26 July 1991.

REFERENCES

Allison, S. A., J. C. Herr, and J. M. Schurr. 1981. Structure of virial ϕ29 DNA condensed by simple triamines: a light-scattering and electron-microscopy study. *Biopolymers.* 20:469–488.

Bloomfield, V. A., R. W. Wilson, and D. C. Rau. 1980. Comparison of polyelectrolyte theories of binding of cations to DNA. *Biophys. Chem.* 11:339–343.

Brenner, S. L., and D. A. McQuarrie. 1973. Force balances in systems of cylindrical polyelectrolytes. *Biophys. J.* 13:301–331.

Cevc, G., R. Podgornik, and B. Zeks. 1982. The free energy, enthalpy, and entropy of phospholipid bilayer membranes and their dependence on the interfacial separation. *Chem. Phys. Lett.* 91:193–196.

Chattoraj, D. K., L. C. Gosule, and J. A. Schellman. 1978. DNA condensation with polyamines II. Electron microscopic studies. *J. Mol. Biol.* 121:327–337.

Gosule, L. C., and J. A. Schellman. 1978. DNA condensation with polyamines I. Spectroscopic studies. *J. Mol. Biol.* 121:311–326.

Gruen, D. W. R., S. Marcelja, and V. A. Parsegian. 1984. Water structure near the membrane surface. *In* Cell Surface Dynamics, Concepts and Models. A. Perelson, K. Wiegel, and C. Delisi, editors. Marcel Dekker, New York. 59–91.

Herskovits, T. T., and J. Brahms. 1976. Structural investigations on DNA-protamine complexes. *Biopolymers.* 15:687–706.

Horn, R. G., J. N. Israelachvili, J. Marra, V. A. Parsegian, R. P. Rand. 1988. Comparison of forces measured between phosphatidylcholine bilayers. *Biophys. J.* 54:1185–1187.

Knoll, D. A., M. G. Fried, and V. A. Bloomfield. 1988. Heat-induced DNA aggregation in the presence of divalent metal salts. *In* Structure & Expression, Vol. 2, DNA and Its Drug Complexes. R. H. Sarma and M. H. Sarma, editors. Adenine Press, New York. 123–145.

Kornyshev, A. A., and S. Leikin. 1989. Fluctuation theory of hydration forces: the dramatic effects of inhomogeneous boundary conditions. *Phys. Rev. A* 40:6431–6437.

Leikin, S., D. C. Rau, and V. A. Parsegian. 1991. Measured entropy and enthalpy of water as a function of distance between DNA double helices. *Phys. Rev. A.* 44:5272–5278.

Manning, G. S. 1978. The molecular theory of polyelectrolyte solutions with applications to the electrostatic properties of polynucleotides. *Quart. Rev. Biophys.* 11:179–246.

Marcelja, S., and N. Radic. 1976. Repulsion of interfaces due to boundary water. *Chem. Phys. Lett.* 42:129–130.

McGhee, J. D., and P. H. von Hippel. 1974. Theoretical aspects of DNA-protein interactions: Cooperative and noncooperative binding of large ligands to a one-dimensional homogeneous lattice. *J. Mol. Biol.* 86:469–486.

McGhee, J. D., W. I. Wood, M. Dolan, J. D. Engel, and G. Felsenfeld. 1981. A 200 base pair region at the 5′ end of the chicken adult β-globin gene is accessible to nuclease digestion. *Cell.* 27:45–55.

Mudd, C. P., H. Tipton, V. A. Parsegian, and D. C. Rau. 1987. Temperature-controlled vacuum chamber for x-ray diffraction studies. *Rev. Sci. Instrum.* 58:2110–2114.

Parsegian, V. A., R. P. Rand, and D. C. Rau. 1985. Hydration forces: what next? *Chem. Scr.* 25:28–31.

Parsegian, V. A., R. P. Rand, N. L. Fuller, and D. C. Rau. 1986. Osmotic stress for the direct measurement of intermolecular forces. *Methods Enzymol.* 127:400–416.

Parsegian, V. A., R. P. Rand, and D. C. Rau. 1987. Lessons from the direct measurement of forces between biomolecules. *In* Physics of Complex and Supermolecular Fluids. S. A. Safran and N. A. Clark, editors. John Wiley and Sons, New York. 115–135.

Plum, G. E., and V. A. Bloomfield. 1988. Equilibrium dialysis study of hexammine cobalt (III) to DNA. *Biopolymers.* 27:1045–1051.

Podgornik, R., D. C. Rau, and V. A. Parsegian. 1989. The action of interhelical forces on the organization of DNA double helices: fluctuation-enhanced decay of electrostatic double-layer and hydration forces. *Macromol.* 22:1780–1786.

Podgornik, R., and V. A. Parsegian. 1990. Molecular fluctuations in the packing of polymeric liquid crystals. *Macromol.* 23:2265–2269.

Post, C. B., and B. H. Zimm. 1979. Internal condensation of a single DNA molecule. *Biopolymers.* 18:1487–1501.

Prouty, M. S., A. N. Schechter, and V. A. Parsegian. 1985. Chemical potential measurements of deoxyhemoglobin S polymerization: determination of the phase diagram of an assembling protein. *J. Mol. Biol.* 184:517–528.

Rand, R. P. 1981. Interacting phospholipid bilayers: measured forces and induced structural changes. *Annu. Rev. Biophys. Bioeng.* 10:277–314.

Rand, R. P., N. Fuller, V. A. Parsegian, and D. C. Rau. 1988. Variation in hydration forces between neutral phospholipid bilayers: evidence for hydration attraction. *Biochemistry.* 27:7711–7722.

Rand, R. P., and V. A. Parsegian. 1989. Hydration forces between phospholipid bilayers. *Biochim. Biophys. Acta.* 988:351–376.

Rand, R. P., N. L. Fuller, S. M. Gruner, and V. A. Parsegian. 1990. Membrane curvature, lipid segregation, and structural transitions for phospholipids under dual-solvent stress. *Biochemistry.* 29:76–87.

Rau, D. C., B. K. Lee, and V. A. Parsegian. 1984. Measurement of the repulsive force between polyelectrolyte molecules in ionic solution:

hydration forces between parallel DNA double helices. *Proc. Natl. Acad. Sci. USA.* 81:2621–2625.

Rau, D. C., and V. A. Parsegian. 1992. Direct measurement of temperature-dependent solvation between DNA double helices. *Biophys. J.* 61:260–271.

Rau, D. C., and V. A. Parsegian. 1990. Direct measurement of forces between linear polysaccharides: Xanthan and schizophyllan. *Science (Wash. DC).* 249:1278–1281.

Record, M. T., C. F. Anderson, and T. M. Lohman. 1978. Thermodynamic analysis of ion effects on the binding and conformational equilibria of proteins and nucleic acids: the roles of ion association or release, screening, and ion effects on water activity. *Quart. Rev. Biophys.* 11:103–178.

Schellman, J. A., and N. Parthasarathy. 1984. X-ray diffraction studies on cation-collapsed DNA. *J. Mol. Biol.* 175:313–329.

Suau, P., and J. A. Subirana. 1977. X-ray diffraction studies of nucleoprotamine structure. *J. Mol. Biol.* 117:909–926.

Suwalsky, M., and W. Traub. 1972. A comparative x-ray study of a nucleoprotamine and DNA complexes with polylysine and polyarginine. *Biopolymers.* 11:2223–2231.

Widom, J., and R. L. Baldwin. 1980. Cation-induced toroidal condensation of DNA: studies with $Co^{3+}(NH_3)_6$. *J. Mol. Biol.* 144:431–453.

Widom, J., and R. L. Baldwin. 1983. Monomolecular condensation of λ-DNA induced by cobalt hexammine. *Biopolymers.* 22:1595–1620.

Wilson, R. W., and V. A. Bloomfield. 1979. Counterion-induced condensation of deoxyribonucleic acid. A light scattering study. *Biochemistry.* 18:2192–2196.

Zimmerberg, J., and V. A. Parsegian. 1986. Polymer inaccessible volume changes during opening and closing of a voltage-dependent ionic channel. *Nature (Lond.).* 323:36–39.